



Research paper

Direct synthesis of mesoporous aluminosilicates from Indonesian kaolin clay without calcination



Imroatul Qoniah^{a,b}, Didik Prasetyoko^{b,*}, Hasliza Bahruji^c, Sugeng Triwahyono^d, Aishah Abdul Jalil^d, Suprpto^b, Hartati^e, Tri Esti Purbaningtiast^f

^a Department of Environmental Engineering, Islamic University of Jember, Jl. Kaliurang Km. 14.5, Sleman 55584, Yogyakarta, Indonesia

^b Department of Chemistry, Faculty of Mathematics and Natural Sciences, Institut Teknologi Sepuluh Nopember, Keputih, Sukolilo, Surabaya 60111, Indonesia

^c Cardiff Catalysis Institute, Cardiff University, CF10 3AT Cardiff, United Kingdom

^d Ibnu Sina Institute for Fundamental Science Studies, Universiti Teknologi Malaysia, Skudai, Johor Bahru 81310, Malaysia

^e Department of Chemistry, Faculty of Science and Technology, Universitas Airlangga, Surabaya 60115, Indonesia

^f Diploma of Analytical Chemistry, Islamic University of Jember, Jl. Kaliurang Km. 14.5, Sleman 55584, Yogyakarta, Indonesia

ARTICLE INFO

Article history:

Received 30 March 2015

Received in revised form 25 September 2015

Accepted 7 October 2015

Available online 23 October 2015

Keywords:

Kaolin

Mesoporous

Aluminosilicates based-materials

Surface acidity

ABSTRACT

The transformation of kaolin to amorphous mesoporous aluminosilicate was investigated in this study. We demonstrated the use of kaolin as silica and alumina sources without prior pretreatment. Two steps synthesis method were carried out; hydrothermal reaction at 80 °C, followed by addition of mesoporegen cetyltrimethylammonium bromide (CTABr) surfactant. We observed that prolonging the synthesis period improves the surface area of the aluminosilicate with enhances mesopore volume and surface acidity.

© 2015 Elsevier B.V. All rights reserved.

1. Introduction

There is a growing challenge for developing robust materials based on aluminosilicate framework mainly to be used as catalyst for the synthesis of fine chemicals. Considerable effort has been dedicated to achieve desired mesoporous aluminosilicate materials with high surface area and hydrothermal stability as acid catalyst. Mesoporous structure in aluminosilicate is beneficial in catalytic application; the unique mesopores improve the mass transport and the diffusion of chemical reactant that subsequently accelerates the catalytic process (Pérez-Ramírez et al., 2008). Mass transport is faster in the catalyst cavity that offers shorter diffusion pathway between the reactant and the active site of the catalyst (Na et al., 2013).

Although the synthesis of aluminosilicates are well-established, commercial silica and alumina for example tetraethylorthosilicate (Li et al., 2013; Enterría et al., 2014; Li et al., 2010), colloidal silica (Xue et al., 2012), aluminum isopropoxide (Rownaghi et al., 2012; Jian et al., 2013), aluminum nitrate nonahydrate (Gonçalves et al., 2008) and sodium aluminate (Petushkov et al., 2011; Liu et al., 2014) are often used as starting material. Natural minerals provides alternative green and sustainable silica and alumina sources to replace the used of

synthetic chemicals. Many researchers have explored the potential of silica from rice husk ash (Prasetyoko et al., 2012), palygorskite (Jiang et al., 2014), and kaolin (Pan et al., 2013) for aluminosilicate synthesis. However, these materials must undergo calcination and acid leaching pretreatment to eliminate impurities that have significant influences on the physical properties of the synthesized materials. Kaolin is a clay mineral with the chemical composition of $\text{Al}_2\text{Si}_2\text{O}_5(\text{OH})_4$. It consists of high Si and Al contents that is beneficial for aluminosilicate synthesis. The Si and Al in kaolin however exist in inactive states, which make the transformation into aluminosilicate is a challenging process (Chandrasekhar and Pramada, 2008). Conversion of kaolin into silica-based materials such as Ln-ZSM-5/MCM-41 (Li et al., 2010), mesoporous Al_2O_3 (Liu and Yang, 2010; Pan et al., 2013), Al-MCM-41 (Du and Yang, 2012) requires calcination at high temperature to activate the kaolin. Soft-template such as surfactant is added into the gel mixture or after crystallization period, which control the pore structure and the particle size of the intercrystalline powder (Li et al., 2013; Enterría et al., 2014).

Here, we report direct synthesis of amorphous mesoporous aluminosilicate using raw kaolin clay as the Si and Al sources without prior pre-treatment. Silicalite-1 seed was used as structure-directing agent (SDA) to obtain MFI-type framework, while cationic surfactant, CTABr was used as mesoporegen. We studied the transformation of kaolin into mesoporous aluminosilicate by monitoring the changes in porosity,

* Corresponding author.

E-mail addresses: didikp@chem.its.ac.id, didik.prasetyoko@gmail.com (D. Prasetyoko).

acidity and surface area of the synthesized materials at various hydrothermal synthesis periods.

2. Experimental

2.1. Materials

Mesoporous aluminosilicate was prepared by kaolin (kaolinite, $\text{Al}_4(\text{Si}_4\text{O}_{10})(\text{OH})_8$) from Bangka Belitung, Indonesia with the composition of (wt%) Al_2O_3 (22%), SiO_2 (57%), P_2O_5 (3.9%), K_2O (3.22%), CaO (1.8%), TiO_2 (2.2%), V_2O_5 (0.15%), Fe_2O_3 (8.89%), CuO (0.31%), Ga_2O_3 (0.074%), ZrO_2 (0.22%), and BaO (0.77%); NaOH (sodium hydroxide, pelet, Applichem, >99.5%); LUDOX (colloidal silica, SiO_2 , Aldrich, 30%); distilled water; CTABr (cetyltrimethylammonium bromide, $\text{C}_{19}\text{H}_{42}\text{BrN}$, Applichem, 99%); and seed silicalite-1.

2.2. Synthesis

For the synthesis of mesoporous aluminosilicate, kaolin (3.7 g) was mixed thoroughly with NaOH solution (3.2 g in 40 mL of distilled water) followed by gradual addition of ludox (73 g) to the mixture. The mixture was stirred for 15 min before 40 ml of distilled water was added to give final chemical composition ratios of $10 \text{ Na}_2\text{O} : 100 \text{ SiO}_2 : 2 \text{ Al}_2\text{O}_3 : 1800 \text{ H}_2\text{O}$ (Prasetyoko et al., 2012). The stirring was continued for 8 h to obtain gel mixture and leave to age for another 12 h. The silicalite-1 seed (0.29 g) was subsequently added to the mixture followed by 30 min stirring.

The resulting mixture was then transferred into stainless steel autoclave and placed in oven at 80°C for 12, 24 and 48 h. The autoclave was brought immediately to room temperature by quenching with cold water. The CTABr (12.6 g, $\text{SiO}_2/\text{CTABr} = 3.85$) were slowly added and stirred for 1 h to obtain homogenous gel. The mixture was left to age at room temperature for 4 h. The solid products were separated by centrifugation (5000 rpm) and thoroughly washed with distilled water until the pH of supernatant is neutral. The final product was dried at 60°C for 24 h. The resulting powder was calcined at 550°C under continuous flow of N_2 for 1 h, followed by air calcination for another 6 h.

2.3. Characterization

X-ray powder diffraction patterns of crystal phase were recorded on a Philips Expert with $\text{Cu K}\alpha$ (40 kV, 30 mA) radiation in the range $2\theta = 5\text{--}40^\circ$. The infrared spectra (range $400\text{--}1400 \text{ cm}^{-1}$) of characteristic

vibration bands were monitored by FTIR Shimadzu Instrument Spectrum One 8400S. Total surface area, pore size distribution and total pore volume were determined from N_2 adsorption-desorption using a Quantachrome Instruments Nova 1200. Total surface area was determined by the BET and pore size distribution and volume in the mesopore were determined from the BJH method. The t -plot method was employed to calculate the micro-mesopore surface area and micropore volume while HK method was applied to calculate the pore size distribution in the micropore range. The acidity was measured by pyridine adsorption using FTIR spectrometer. Samples (13 mg) were pressed into wafer, placed in the homemade glass transmission cell and outgassed at 400°C for 3 h under N_2 flow. Pyridine was adsorbed at room temperature for 1 h and subsequently evacuated at 150°C for 3 h. FTIR Spectra were recorded in the $1600\text{--}1400 \text{ cm}^{-1}$. For TEM images, high resolution images and selected area electron diffraction patterns were recorded using a JEM 1400 instrument operating at 120 kV.

3. Results and discussion

XRD patterns of fresh kaolin and amorphous mesoporous aluminosilicates produced after 12, 24, and 48 h of crystallization period are shown in Fig. 1A. As observed, the kaolin precursor consists of a well-crystallized kaolinite. For the synthesized mesoporous aluminosilicates, the diffraction patterns consist of a big hump at $2\theta = 20\text{--}30^\circ$ indicating the amorphous aluminosilicate framework, as reported by Du and Yang (2012) and Dang et al. (2013). The transformation of kaolin crystalline phase to amorphous aluminosilicate have occurred at ~ 12 h of hydrothermal synthesis which the process presumably involves the dissolution of kaolin sheet-structure of amorphous silica (Chandrasekhar and Pramada, 2008; Liu and Yang, 2010).

We used infrared spectroscopy analysis to investigate the transformation of kaolin to mesoporous aluminosilicates framework. The infrared spectra of the fresh kaolin shows band appeared at $428, 470$ and 541 cm^{-1} which are corresponded to the vibrations of Si-O-Al framework. The bands appeared at $696, 754$ and 790 cm^{-1} were assigned to the vibrations of gibbsite-like layers of kaolinite. Peak at 917 cm^{-1} is Al-OH vibration and the peaks at 1033 , and 1110 cm^{-1} are the vibrations of in plane Si-O stretching (Olejnik et al., 1968; Dang et al., 2013) (Fig. 1B). Product obtained after 12 h of synthesis shows the peaks corresponded to kaolinite has disappeared together with the appearance of the peaks at $1090, 796$, and 470 cm^{-1} that were characteristics of the silica-based materials framework. The shoulder peaks at

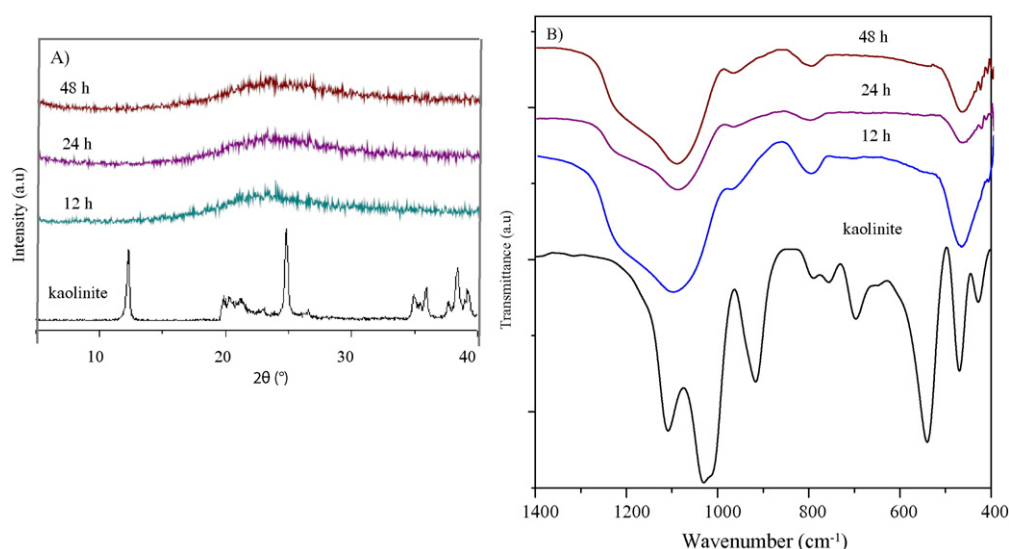


Fig. 1. A) XRD pattern and B) FTIR spectra of the synthesized amorphous mesoporous aluminosilicates at 12, 24 and 48 h.

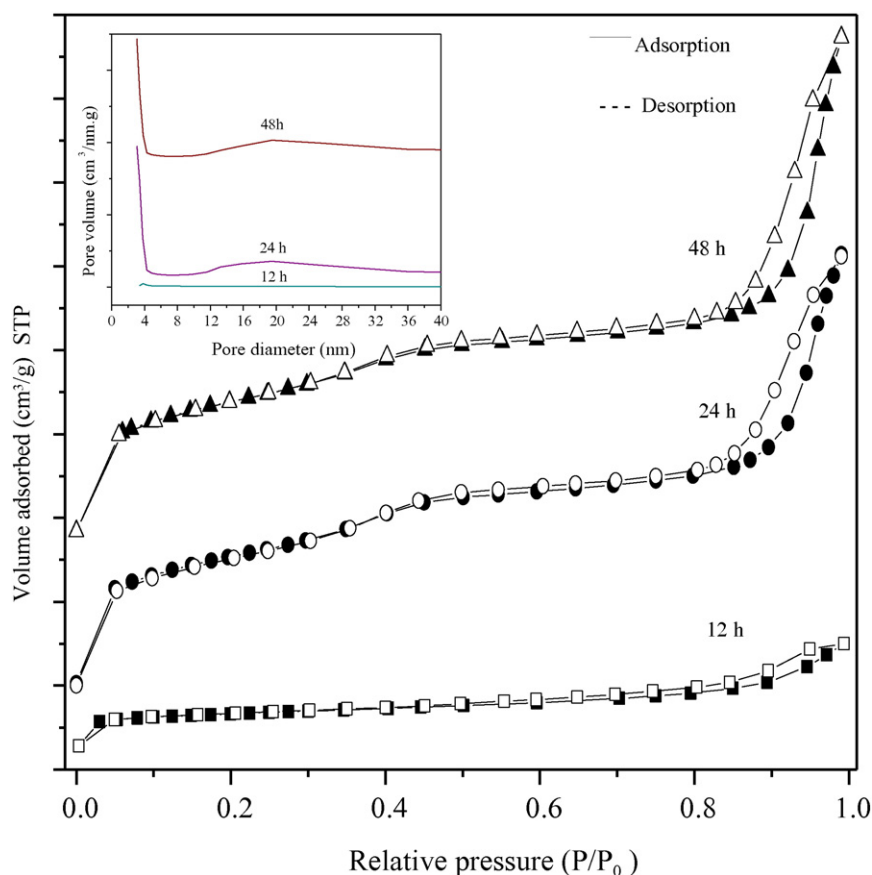


Fig. 2. N_2 adsorption/desorption isotherms of amorphous mesoporous aluminosilicates at 12, 24 and 48 h of hydrothermal synthesis.

$\sim 1220 \text{ cm}^{-1}$ was assigned to the external asymmetry stretching of Si–O–Si bond and the peak at 960 cm^{-1} was attributed to the terminal silanol groups (Si–OH) on the wall surface of the mesopores (Gonçalves et al., 2008). There is no significant change in the infrared spectra of the solid product when the hydrothermal synthesis was extended to 24 and 48 h suggesting that the aluminosilicates framework has entirely formed after 12 h of hydrothermal crystallizations.

The N_2 adsorption-desorption isotherms of the synthesis of mesoporous aluminosilicates have been carried out to determine the specific surface area, the pore size distribution, the total pore volume and the pore structure of the synthesized materials. The isotherms adsorption characteristics of the solid products after hydrothermal synthesis are shown in Fig. 2. The isotherm adsorption from the aluminosilicate obtained after 12 h indicates the type I isotherms based on the evidence of gas adsorption at low relative pressure ($P/P_0 < 0.3$) and the absence of hysteresis loop. The calculated micropore surface area is significantly higher $\sim 58 \text{ m}^2/\text{g}$ relative to the total surface area of the synthesis materials $\sim 66 \text{ m}^2/\text{g}$ (Table 1). Meanwhile, for aluminosilicates synthesized

for 24 h and 48 h, the isotherms adsorption patterns illustrate the type IV isotherm with the presence of hysteresis loop ($P/P_0 = 0.3\text{--}1.0$) due to the capillary condensation processes, which is a characteristic of mesoporous material. The micropore and mesopore surface area calculated from the isotherms data was given in Table 1. The BET surface area of aluminosilicates synthesized for 24 h is $531 \text{ m}^2/\text{g}$, while t-plot micropore and mesopore surface area are $333 \text{ m}^2/\text{g}$ and $198 \text{ m}^2/\text{g}$, respectively. Solid product obtained after 48 h of hydrothermal synthesis, produced aluminosilicate with the surface area of $545 \text{ m}^2/\text{g}$, the micropore surface area of $375 \text{ m}^2/\text{g}$, and the mesopore surface area of $170 \text{ m}^2/\text{g}$. This result indicates the aluminosilicate may consist of a mixture of microporous and mesoporous intercrystalline structure. This finding (both type I and IV in one sample) was similar to the adsorption isotherm reported by Petushkov et al. (2011).

Table 1 summarized the physical characterization of the aluminosilicate calculated from the analysis of N_2 adsorption data. The specific surface area of the aluminosilicate increases significantly when the hydrothermal synthesis was extended from 12 h to 24 h. However,

Table 1
Physical and acidity properties of amorphous mesoporous aluminosilicates synthesized directly from kaolin.^a

Sample name	S_{BET}^a (m^2/g)	Surface areas ^b (m^2/g)		V_{meso}^c ($\text{cm}^3/\text{g}^{-1}$)	V_{micro}^b ($\text{cm}^3/\text{g}^{-1}$)	D_{meso}^c (nm) ^c		D_{micro}^d (nm) ^d	Number of acid site (mmol/g) ^e	
		S_{meso}	S_{micro}			Small	Large		Brønsted	Lewis
12 h	66	7	58	0.08	0.02	3.81	–	0.65	0.07	0.09
24 h	531	333	198	0.71	0.09	3.07	19.5	1.40	0.31	0.34
48 h	545	375	170	0.85	0.06	3.05	19.5	1.39	0.60	0.41

^a S_{BET} (Total surface area) by BET method.

^b S_{meso} (mesopore surface areas), S_{micro} (micropore surface areas), V_{micro} (micropore volume) by t-plot method.

^c V_{meso} (mesopore volume), D_{meso} (mesopore diameter or distribution) by BJH method.

^d D_{micro} (micropore diameter) by HK method.

^e B and L acid sites by pyridine adsorption.

prolonging the hydrothermal treatment to 48 h only shows a small enhancement of surface area. We however found that the specific surface area of the mesopores improves with longer crystallization period with the surface area of the micropores suffers a slight reduction at 48 h. Similar trend was found on the pore diameter and the volume of mesoporous and micropores structures. As shown in Fig. 2 (inset) and Table 1, all aluminosilicates have micropore diameter in the range of 0.65 and 1.40 nm. However, the pore size distribution of sample synthesized for 24 and 48 h presents bimodal porosity of mesopore i.e. 3 and 19 nm with very intense peak (Fig. 2: BJH pore size distribution). On the contrary, the sample synthesized for 12 h only indicates mesopore diameter about 3 nm with very small peak. This shows that hydrothermal treatment at longer period of time facilitates the formation of mesopores structures in the aluminosilicate framework (Enterría et al., 2014; Petushkov et al., 2011).

Mesoporous aluminosilicate is known as active acid catalyst, therefore it is beneficial to determine the acidity of the synthesized materials and the effect of the crystallization time on the number of acid sites on the surface. Pyridine adsorption studies are useful to determine the acidity of the mesoporous silicate. This method is able to distinguish between the Brønsted (B) and Lewis (L) acid sites (Emeis, 1993). The pyridine adsorption infrared analysis of aluminosilicates after 12 h of synthesis illustrated in Fig. 3 shows a very small peak of adsorbed pyridine. The peaks corresponded to the Brønsted and the Lewis acid sites at ~ 1540 and 1450 cm^{-1} were detected for the aluminosilicates samples with the intensity increases with the crystallization time at 24 and 48 h (Fig. 3). Peak appeared at 1490 cm^{-1} in all samples is a characteristic for both Brønsted and Lewis acid sites. The number of acid sites were calculated based on the area of pyridine adsorption peak and were summarized in Table 1. It is clear that the crystallization period affects the number of acid sites particularly for Brønsted sites, where the value increases from 0.07 to 0.31 to 0.60 mmol/g at 12, 24 and 48 h, respectively. The result suggests that although the kaolin loses its crystalline structure and presumably form aluminosilicates framework after 12 h of crystallization period, longer hydrothermal treatment is crucial to form the mesoporous structure and to increase the number of acid sites on the surface. The number of Brønsted acid sites enhances with the hydrothermal crystallization time. This is as a result of the greater number of tetrahedrally-coordinated aluminum in the aluminosilicate mesoporous solids (Jian et al., 2013).

The particle size and the formation of mesoporous aggregates was controlled by the reaction conditions, such as synthesis time, pH and addition of structure directing agent (Petushkov et al., 2011). The TEM analysis on the synthesized product at 48 h revealed the morphology of the mesoporous aluminosilicate. Fig. 4 shows the synthesis powder consists of nanoparticles aggregates with uniform particle size of $\sim 40\text{ nm}$

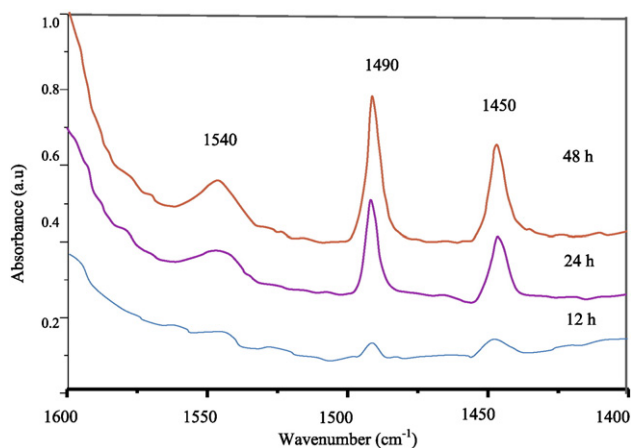


Fig. 3. Pyridine-FTIR spectra of amorphous mesoporous aluminosilicates synthesized directly from kaolin after adsorption of pyridine and evacuation at $150\text{ }^{\circ}\text{C}$ for 3 h.

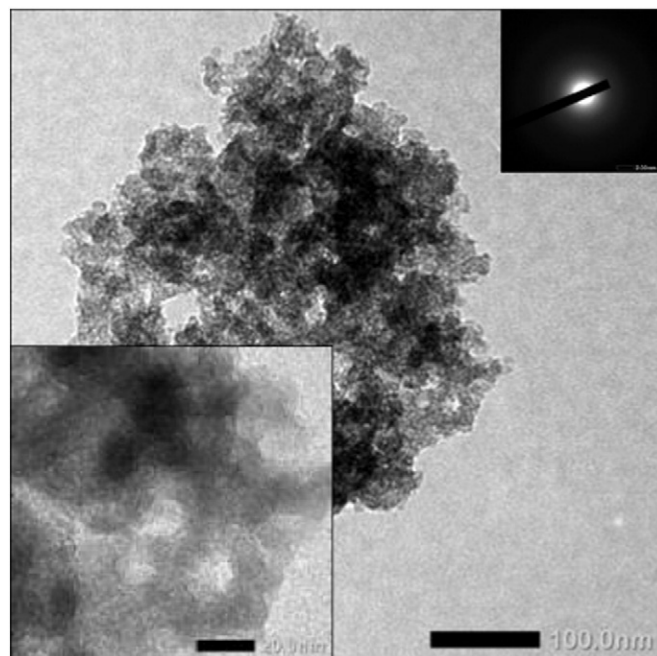


Fig. 4. TEM images of synthesized amorphous mesoporous aluminosilicates at 48 h.

without identical orientation. The SAED (Selected Area Diffraction) analysis confirms the amorphous structure of the aluminosilicates.

4. Conclusions

Amorphous mesoporous aluminosilicate was synthesized from raw kaolin as Si and Al sources using hydrothermal and soft-templating methods. The properties of the synthesized aluminosilicates exhibit the mesopore and micropore within the structure with high surface area and acidity. We observed the importance of extending the crystallization period to 24 h for formation of aluminosilicate with high surface area, mesopore volume and surface acidity.

Acknowledgments

The authors would like to acknowledge the Ministry of Research and Higher Education, Indonesia, under “PUPT” research grant No. 003246.18/IT2.11/PN.08/2015.

References

- Chandrasekhar, S., Pramada, P.N., 2008. Microwave assisted synthesis of zeolite A from metakaolin. *Microporous Mesoporous Mater.* 108, 152–161.
- Dang, T.H., Chen, B., Lee, D.J., 2013. Application of kaolin-based catalysts in biodiesel production via transesterification of vegetable oils in excess methanol. *Bioresour. Technol.* 145, 175–181.
- Du, C., Yang, H., 2012. Investigation of the physicochemical aspects from natural kaolin to Al-MCM-41. *J. Colloid Interface Sci.* 369, 216–222.
- Emeis, C.A., 1993. Determination of integrated molar extinction coefficients for infrared absorption bands of pyridine adsorbed on solid acid catalysts. *J. Catal.* 141, 347–354.
- Enterría, M., Suárez-García, F., Martínez-Alonso, A., Tascón, J.M.D., 2014. Preparation of hierarchical micro-mesoporous aluminosilicate composites by simple Y zeolite/MCM-48 silica assembly. *J. Alloys Compd.* 58, 60–69.
- Gonçalves, M.L., Dimitrov, L.D., Jordão, M.H., Wallau, M., Urquieta-González, E.A., 2008. Synthesis of mesoporous ZSM-5 by crystallisation of aged gels in the presence of cetyltrimethylammonium cations. *Catal. Today* 133–135, 69–79.
- Jian, Z., Zhicheng, L., Liyuan, L., Yangdong, W., Huanxin, G., Weimin, Y., Zaiku, X., Yi, T., 2013. Hierarchical mesoporous ZSM-5 zeolite with increased external surface acid sites and high catalytic performance in O-xylene isomerization. *Chin. J. Catal.* 34, 1429–1433.
- Jiang, J., Duanmu, C., Yanga, Y., Gua, X., Chen, J., 2014. Synthesis and characterization of high siliceous ZSM-5 zeolite from acid-treated palygorskite. *Powder Technol.* 251, 9–14.

- Li, X., Li, B., Xu, J., Wang, Q., Pang, X., Gao, X., Zhou, Z., Piao, J., 2010. Synthesis and characterization of Ln-ZSM-5/MCM-41 (Ln = La, Ce) by using kaolin as raw material. *Appl. Clay Sci.* 50, 81–86.
- Li, H., Wu, H., Shi, J., 2013. Competition balance between mesoporous self-assembly and crystallization of zeolite: a key to the formation of mesoporous zeolite. *J. Alloys Compd.* 556, 71–78.
- Liu, M., Yang, H., 2010. Large surface area mesoporous Al₂O₃ from kaolin: methodology and characterization. *Appl. Clay Sci.* 50, 554–559.
- Liu, B., Zheng, L., Zhu, Z., Li, C., Xi, H., Qian, Y., 2014. Hierarchically structured Beta zeolites with intercrystal mesopores and the improved catalytic properties. *Appl. Catal. A Gen.* 470, 412–419.
- Na, K., Choi, M., Ryoo, R., 2013. Recent advances in the synthesis of hierarchically nanoporous zeolites. *Microporous Mesoporous Mater.* 166, 3–19.
- Olejnik, S., Aylmore, L.A.G., Posner, A.M., Quirk, J.P., 1968. Infrared spectra of kaolin mineral dimethyl sulfoxide complexes. *J. Phys. Chem.* 72, 241–249.
- Pan, F., Lu, X., Wang, T., Wang, Y., Zhang, Z., Yan, Y., Yang, S., 2013. Synthesis of large-mesoporous γ -Al₂O₃ from coal-series kaolin at room temperature. *Mater. Lett.* 91, 136–138.
- Pérez-Ramírez, J., Christensen, C.H., Egeblad, K., Christensen, C.H., Groen, J.C., 2008. Hierarchical zeolites: enhanced utilisation of microporous crystals in catalysis by advances in materials design. *Chem. Soc. Rev.* 37, 2530–2542.
- Petushkov, A., Yoon, S., Larsen, S.C., 2011. Synthesis of hierarchical nanocrystalline ZSM-5 with controlled particle size and mesoporosity. *Microporous Mesoporous Mater.* 137, 92–100.
- Prasetyoko, D., Ayunanda, N., Fansuri, H., Hartanto, D., 2012. Phase transformation of rice husk ash in the synthesis of ZSM-5 without organic template. *J. Math. Fund. Sci.* 44 A (3), 250–262.
- Rownaghi, A.A., Rezaei, F., Hedlund, J., 2012. Uniform mesoporous ZSM-5 single crystals catalyst with high resistance to coke formation for methanol deoxygenation. *Microporous Mesoporous Mater.* 151, 26–33.
- Xue, T., Chen, L., Wang, Y.M., He, M.Y., 2012. Seed-induced synthesis of mesoporous ZSM-5 aggregates using tetrapropylammonium hydroxide as single template. *Microporous Mesoporous Mater.* 156, 97–105.